Letter

Interacting electrons and bosons in the doubly screened $G\widetilde{W}$ approximation: A time-linear scaling method for first-principles simulations

Y. Pavlyukh,[1,2] E. Perfetto,[2,3] and G. Stefanucci[2,3]
[1]*Department of Theoretical Physics, Faculty of Fundamental Problems of Technology, Wrocław University of Science and Technology, 50-370 Wrocław, Poland*
[2]*Dipartimento di Fisica, Università di Roma Tor Vergata, Via della Ricerca Scientifica 1, 00133 Rome, Italy*
[3]*INFN, Sezione di Roma Tor Vergata, Via della Ricerca Scientifica 1, 00133 Rome, Italy*

(Received 15 March 2022; revised 5 July 2022; accepted 9 November 2022; published 30 November 2022)

We augment the time-linear formulation of the Kadanoff-Baym equations for systems of interacting electrons and quantized phonons or photons with the $G\widetilde{W}$ approximation, the Coulomb interaction $\widetilde{W}$ being dynamically screened by both electron-hole pairs *and* bosonic particles. We also show how to combine different approximations to include simultaneously multiple correlation effects in the dynamics. The final outcome is a versatile framework comprising 2^{12} distinct diagrammatic methods, each scaling linearly in time and preserving all fundamental conservation laws. The dramatic improvement over current state-of-the-art approximations brought about by $G\widetilde{W}$ is demonstrated in a study of the correlation-induced charge migration of the glycine molecule in an optical cavity.

DOI: 10.1103/PhysRevB.106.L201408

Introduction. After Feynman's visionary idea in 1949 [1], the Green's function (GF) diagrammatic theory developed into a powerful and versatile approach in nearly every field of theoretical physics. In condensed-matter theory [2–5], efforts toward the nonequilibrium extension of the formalism (NEGF) [6,7] culminated in the so-called Kadanoff-Baym equations (KBE) [8,9]. The KBE govern the dynamics of correlated electrons and bosons and give access to the electronic, magnetic, and optical properties of any quantum system, from simple molecules to bulk materials. As for any exact reformulation of the many-body Schrödinger equation, the applicability of the KBE relies on accurate approximations and efficient implementation schemes [10–13].

In Ref. [14] we built on the generalized Kadanoff-Baym ansatz (GKBA) for electrons [15] and bosons [16] and on the time-linear formulation of the GKBA-KBE with electron-electron (*e-e*) [17,18] and electron-boson (*e-b*) [16] interactions to map a broad class of NEGF approximations onto a coupled system of ordinary differential equations (ODEs). Available methods to treat *e-e* correlations include *GW* [19], *T*-matrix (either without or with exchange) and Faddeev [20], while *e-b* correlations are described by Ehrenfest and second-order diagrams in the *e-b* coupling [21–24]. Every method in this NEGF toolbox guarantees the fulfillment of all fundamental conservation laws [9,25,26].

In this work we present a substantial advance in the treatment of correlations, requiring no extra computational cost and preserving all conserving properties. Specifically, we include the effects of dynamical screening due to *both* *e-e* and *e-b* interactions ($G\widetilde{W}$ approximation) [27,28]. The $G\widetilde{W}$ extension opens the door to a wealth of phenomena, ranging from carrier relaxation [29,30] and exciton recombination [31,32] to molecular charge migration and transfer in optical or plasmonic cavities [33–36]. We further show how to combine different methods without incurring any double counting. The final outcome is a NEGF toolbox that can be used to investigate the correlated dynamics of electrons and bosons in 2^{12} distinct diagrammatic approximations. Real-time simulations of the correlation-induced charge migration of the glycine molecule in an optical (or plasmonic) cavity demonstrates the superiority of the $G\widetilde{W}$ method over other approximations.

Preliminaries. We consider a system of electrons with one-particle time-dependent Hamiltonian $h_{ij}(t)$ and *e-e* interaction v_{ijmn} (Latin indices $i, j, \ldots$ etc. specify the spin orbitals of an orthonormal basis) coupled linearly to the displacement $\hat{\phi}_{\boldsymbol{\mu},1} \equiv \hat{x}_{\boldsymbol{\mu}} = (\hat{a}^\dagger_{\boldsymbol{\mu}} + \hat{a}_{\boldsymbol{\mu}})/\sqrt{2}$ and momentum $\hat{\phi}_{\boldsymbol{\mu},2} = \hat{p}_{\boldsymbol{\mu}} = i(\hat{a}^\dagger_{\boldsymbol{\mu}} - \hat{a}_{\boldsymbol{\mu}})/\sqrt{2}$ of a set of bosonic modes of frequency $\omega_{\boldsymbol{\mu}}$. Introducing the Greek index $\mu = (\boldsymbol{\mu}, \xi)$ with $\xi = 1, 2$, we denote by $g_{\mu,ij}$ the interaction strength of the *e-b* coupling. The equation of motion (EOM) for the one-electron density matrix $\rho^<_{ij}(t) \equiv \langle \hat{d}^\dagger_j(t)\hat{d}_i(t)\rangle$ [with $\hat{d}^{(\dagger)}$'s the electronic annihilation (creation) operators] and one-boson density matrix $\gamma^<_{\mu\nu}(t) \equiv \langle \Delta\hat{\phi}_\nu(t)\Delta\hat{\phi}_\mu(t)\rangle$ [with $\Delta\hat{\phi}_\nu \equiv \hat{\phi}_\nu - \langle\hat{\phi}_\nu\rangle$ the bosonic fluctuation operator] reads [16]

$$i\frac{d}{dt}\rho^<(t) = [h^e(t), \rho^<(t)] - i(I^e(t) + I^{e\,\dagger}(t)), \tag{1a}$$

$$i\frac{d}{dt}\boldsymbol{\gamma}^<(t) = [\boldsymbol{h}^b(t), \boldsymbol{\gamma}^<(t)] + i(\boldsymbol{I}^b(t) + \boldsymbol{I}^{b\dagger}(t)), \tag{1b}$$

where $h^e_{ij}(t) = h_{ij}(t) + \sum_{mn}[v_{imnj}(t) - v_{imjn}(t)]\rho^<_{nm}(t) + \sum_\mu g_{\mu,ij}(t)\phi_\mu(t)$ is the mean-field electronic Hamiltonian [$\phi_\mu = \langle\hat{\phi}_\mu\rangle$ for brevity], whereas $\boldsymbol{h}^b(t) = 2\boldsymbol{\alpha}\boldsymbol{\Omega}(t)$, with $\alpha_{\mu\mu'} \equiv \delta_{\boldsymbol{\mu}\boldsymbol{\mu}'}\begin{pmatrix}0 & i\\ -i & 0\end{pmatrix}_{\xi\xi'}$ and $\Omega_{\mu\mu'}(t) \equiv \frac{1}{2}\delta_{\mu\nu}\omega_{\boldsymbol{\mu}}(t)$, is the free-boson Hamiltonian. To distinguish matrices in the one-electron space from matrices in the one-boson space we use boldface for the latter. The time dependence of the *e-e* coupling $v_{ijmn}(t)$ and *e-b* coupling $g_{\mu,ij}(t)$ could be due to the adiabatic switching protocol adopted to generate a correlated initial state [37], whereas the time dependence of the one-particle Hamiltonian $h_{ij}(t)$ and bosonic frequencies $\omega_{\boldsymbol{\mu}}(t)$ could be due to some external field, e.g., laser fields [38,39], phonon drivings [40], etc. As the mean-field Hamiltonian h^e depends on $\phi_\mu(t)$, the EOM (1) must be complemented with the Ehrenfest EOM for the displacements and momenta of the bosonic modes, see below.

The collision integrals I^e and $\boldsymbol{I}^b$ account for all effects beyond mean field. They can be written in terms of two high-order GFs according to [16] $I^e_{lj} = i\sum_{\mu,i} g_{\mu,li}\mathcal{G}^b_{\mu,ij} - i\sum_{imn} v_{lnmi}\mathcal{G}^e_{imjn}$ and $I^b_{\mu\nu} = -i\sum_{\nu,mn}\alpha_{\mu\nu}g_{\nu,mn}\mathcal{G}^b_{\nu,nm}$, where

$$\mathcal{G}^e_{imjn}(t) = -\langle \hat{d}^\dagger_n(t)\hat{d}^\dagger_j(t)\hat{d}_i(t)\hat{d}_m(t)\rangle_c, \tag{2}$$

$$\mathcal{G}^b_{\mu,ij}(t) = \langle \hat{d}^\dagger_j(t)\hat{d}_i(t)\hat{\phi}_\mu(t)\rangle_c. \tag{3}$$

The subscript "c" in the averages signifies that only the correlated part must be retained. The EOM (1) fulfill all fundamental conservation laws if $\mathcal{G}^e$ and $\mathcal{G}^b$ are obtained from the functional derivatives of the correlated part Φ_c of the Baym functional [26] with respect to the *e-e* and *e-b* coupling, respectively, i.e.,

$$\mathcal{G}^e_{imjn}(t) = i\frac{\delta\Phi_c}{\delta v_{jnmi}(t)} + i\frac{\delta\Phi_c}{\delta v_{njim}(t)}, \tag{4a}$$

$$\mathcal{G}^b_{\mu,ij}(t) = \frac{1}{i}\,\frac{\delta\Phi_c}{\delta g_{\mu,ji}(t)}. \tag{4b}$$

In Ref. [16] we have considered the correlated functional $\Phi_c = -½$  – full lines represent electronic GFs G, zigzag lines bosonic GFs D, and empty circles the *e-b* coupling g. The mathematical expression of the considered functional reads (time integrals are over the Keldysh contour)

$$\Phi_c = -\frac{1}{2}\int d\bar{t}d\bar{t}'\,\mathrm{Tr}[\boldsymbol{g}^\dagger(\bar{t})\boldsymbol{D}(\bar{t},\bar{t}')\boldsymbol{g}(\bar{t}')\boldsymbol{\chi}^0(\bar{t}',\bar{t})], \tag{5}$$

where we have defined the matrix $\boldsymbol{g}$ with elements $g_{\mu\nu} = g_{\mu,{j \atop i}} = g_{\mu,ij}$ (hence the second Greek index $\nu = ({j \atop i})$ labels a pair of electronic indices) and the electronic response function $\chi^0_{\mu\nu}(t',t) = \chi^0_{{qj \atop si}}(t',t) \equiv -iG_{qj}(t',t)G_{is}(t,t')$. Consistently with our notation, matrices with Greek indices are represented by boldface letters. Through Eqs. (4) one obtains $\mathcal{G}^e = 0$ and $\boldsymbol{\mathcal{G}}^b(t) = i\int d\bar{t}\boldsymbol{D}(t,\bar{t})\boldsymbol{g}(\bar{t})\boldsymbol{\chi}^0(\bar{t},t^+)$. Implementing the GKBA for electrons and bosons [15,16],

$$G^{\lessgtr}(t,t') = -G^R(t,t')\rho^{\lessgtr}(t') + \rho^{\lessgtr}(t)G^A(t,t'), \tag{6}$$

$$\boldsymbol{D}^{\lessgtr}(t,t') = \boldsymbol{D}^R(t,t')\boldsymbol{\alpha}\boldsymbol{\gamma}^{\lessgtr}(t') - \boldsymbol{\gamma}^{\lessgtr}(t)\boldsymbol{\alpha}\boldsymbol{D}^A(t,t'), \tag{7}$$

one can show that $\boldsymbol{\mathcal{G}}^b$ satisfies a first-order ODE [16] whose coefficients are given by simple functionals of the density matrices $\rho^<$, $\rho^> \equiv \rho^< - 1$ and $\boldsymbol{\gamma}^<$, $\boldsymbol{\gamma}^> \equiv \boldsymbol{\gamma}^< + \boldsymbol{\alpha}$. This is pivotal for constructing a time-linear scheme. The resulting GKBA+ODE are equivalent to the original KBE — in the GKBA framework — with electronic self-energy in the

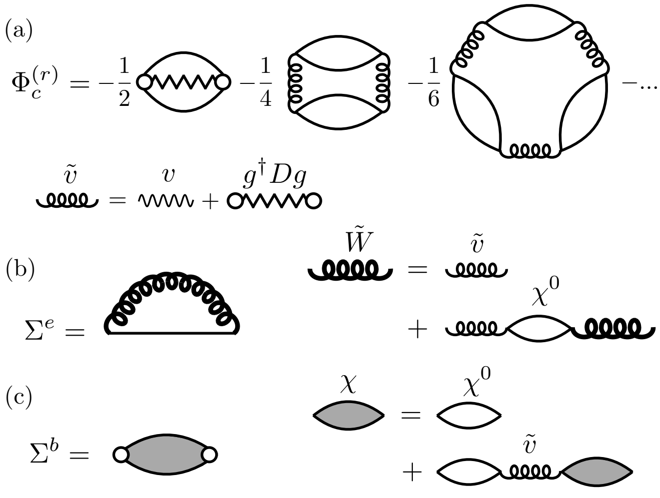

FIG. 1. (a) Diagrams of the reducible $G\widetilde{W}$ functional $\Phi^{(r)}_c$. Full lines are used for G, zigzag lines are used for D, empty circles are used for g, wavy lines are used for v, and gluon lines are used for $\tilde{v}$. (b) Electronic self-energy in terms of the doubly screened interaction $\widetilde{W}$. (c) Bosonic self-energy in terms of the doubly screened response function χ.

GD approximation [23,41,42] and bosonic self-energy proportional to $\boldsymbol{\chi}^0$. The feedback of electrons (bosons) on the bosonic (electronic) subsystem underlies the fulfillment of all conservation laws.

The doubly screened $G\widetilde{W}$ method. The functional Φ_c in Eq. (5) is independent of the *e-e* interaction; hence electronic screening of the *e-b* coupling is not accounted for. This is a severe drawback for extended systems [43,44]. State-of-the-art calculations of electronic lifetimes [45], polaron dispersions [46], and carrier dynamics [30] are indeed performed with a *statically* screened electron-phonon coupling [47–49]. Formally, static screening does not involve any generalization of the *GD* equations: it is sufficient to replace one of the $\boldsymbol{g}$'s in Eq. (5) with $\boldsymbol{g}^s = \boldsymbol{g}(1 + \boldsymbol{\chi}^s\boldsymbol{v})$, where $v_{{im \atop nj}} \equiv v_{ijmn}$ and $\boldsymbol{\chi}^s$ is the random phase approximation (RPA) response function, $\boldsymbol{\chi} = \boldsymbol{\chi}^0 + \boldsymbol{\chi}\boldsymbol{v}\boldsymbol{\chi}^0$, evaluated in equilibrium and at zero frequency. Although $\boldsymbol{g}^s$ is an improvement over the bare $\boldsymbol{g}$, retardation effects and nonequilibrium corrections are still lacking. In the following we show that a time-linear GKBA+ODE scheme can be formulated for the two-times *dynamically* screened coupling $\boldsymbol{g}^d = \boldsymbol{g}(1 + \boldsymbol{\chi}\boldsymbol{v})$.

It is fundamental to observe that the GKBA GFs in Eqs. (6) and (7) are mean-field-like GFs. The theory can therefore be improved in a conserving fashion by calculating $\mathcal{G}^e$ and $\mathcal{G}^b$ from the *reducible* Baym functional $\Phi^{(r)}_c$ [9]. Let $\Phi^{(r)}_c$ be the $G\widetilde{W}$ functional in Fig. 1(a) where $\tilde{\boldsymbol{v}} = \boldsymbol{v} + \boldsymbol{g}^\dagger\boldsymbol{D}\boldsymbol{g}$. This functional is reducible with respect to $\boldsymbol{D}$, but no double counting occurs if $\boldsymbol{D}$ is evaluated from Eq. (7). Remarkably, a time-linear GKBA+ODE scheme can be formulated in this case too. The zeroth-order contribution (in g) is the well-known *GW* approximation, while the second-order contribution corresponds to the aforementioned approximation with dynamically screened $\boldsymbol{g}^d$, and henceforth $G\widetilde{W}^{(2)}$.

The high-order GFs of the doubly screened $G\widetilde{W}$ scheme follow from Eqs. (4) with $\Phi_c^{(r)}$ in place of Φ_c (time integrals are over the Keldysh contour):

$$\boldsymbol{\mathcal{G}}^e(t) = -i\int d\bar{t}d\bar{t}'\,\boldsymbol{\chi}(t,\bar{t})\widetilde{\boldsymbol{v}}(\bar{t},\bar{t}')\boldsymbol{\chi}^0(\bar{t}',t^+), \tag{8a}$$

$$\boldsymbol{\mathcal{G}}^b(t) = i\int d\bar{t}\boldsymbol{D}(t,\bar{t})\boldsymbol{g}(\bar{t})\boldsymbol{\chi}(\bar{t},t^+). \tag{8b}$$

In analogy with $\boldsymbol{\chi}$ and $\boldsymbol{v}$, we have defined $\boldsymbol{\mathcal{G}}^e$ as a matrix in the two-electron space with elements $\mathcal{G}^e_{\mu\nu} = \mathcal{G}^e_{\substack{mj\\ni}} = \mathcal{G}^e_{imjn}$, and in analogy with $\boldsymbol{g}$ we have defined $\boldsymbol{\mathcal{G}}^b$ as a matrix with elements $\mathcal{G}^b_{\mu\nu} = \mathcal{G}^b_{\mu,\substack{j\\i}} = \mathcal{G}^b_{\mu,ij}$. The solution of the EOM (1) with $\boldsymbol{\mathcal{G}}^e$ and $\boldsymbol{\mathcal{G}}^b$ from Eqs. (8) is equivalent to solving the KBE with electronic (nonskeletonic) self-energy $\Sigma^e = -iG\widetilde{W}$, see Fig. 1(b), and bosonic (reducible) self-energy $\boldsymbol{\Sigma}^b = \boldsymbol{g}\boldsymbol{\chi}\boldsymbol{g}^\dagger$, see Fig. 1(c). The nonskeletonicity and reducibility is equivalent to dressing of the GKBA $\boldsymbol{D}$.

The GKBA in Eqs. (6) and (7) can be used to transform $\boldsymbol{\mathcal{G}}^e$ and $\boldsymbol{\mathcal{G}}^b$ into functionals of $\rho^<$ and $\boldsymbol{\gamma}^<$, see Supplemental Material [50], thus closing the EOM for these quantities. Interestingly, however, the EOM for these high-order GFs form a closed system. We separate the two-particle GF into a purely electronic part $\boldsymbol{\mathcal{G}}^{ee} \equiv \boldsymbol{\mathcal{G}}^e|_{g=0}$ (diagrams with no e-b vertices) and a rest $\boldsymbol{\mathcal{G}}^{eb}$, hence $\boldsymbol{\mathcal{G}}^e = \boldsymbol{\mathcal{G}}^{ee} + \boldsymbol{\mathcal{G}}^{eb}$, and show that [50] (omitting the dependence on the time variable)

$$i\frac{d}{dt}\boldsymbol{\mathcal{G}}^{ee} = -\boldsymbol{\Psi}^e + \boldsymbol{h}^e_{\rm eff}\boldsymbol{\mathcal{G}}^{ee} - \boldsymbol{\mathcal{G}}^{ee}\boldsymbol{h}^{e\dagger}_{\rm eff}, \tag{9a}$$

$$i\frac{d}{dt}\boldsymbol{\mathcal{G}}^{eb} = \boldsymbol{\rho}^\Delta\boldsymbol{g}^\dagger\boldsymbol{\mathcal{G}}^b - \boldsymbol{\mathcal{G}}^{b\dagger}\boldsymbol{g}\boldsymbol{\rho}^\Delta + \boldsymbol{h}^e_{\rm eff}\boldsymbol{\mathcal{G}}^{eb} - \boldsymbol{\mathcal{G}}^{eb}\boldsymbol{h}^{e\dagger}_{\rm eff}, \tag{9b}$$

$$i\frac{d}{dt}\boldsymbol{\mathcal{G}}^b = -\boldsymbol{\Psi}^b - \boldsymbol{\alpha}\boldsymbol{g}\boldsymbol{\mathcal{G}}^e - \boldsymbol{\mathcal{A}}\boldsymbol{g}\boldsymbol{\rho}^\Delta + \boldsymbol{h}^b\boldsymbol{\mathcal{G}}^b - \boldsymbol{\mathcal{G}}^b\boldsymbol{h}^{e\dagger}_{\rm eff}, \tag{9c}$$

$$i\frac{d}{dt}\boldsymbol{\mathcal{A}} = \boldsymbol{\mathcal{G}}^b\boldsymbol{g}^\dagger\boldsymbol{\alpha} - \boldsymbol{\alpha}\boldsymbol{g}\boldsymbol{\mathcal{G}}^{b\dagger} + \boldsymbol{h}^b\boldsymbol{\mathcal{A}} - \boldsymbol{\mathcal{A}}\boldsymbol{h}^b, \tag{9d}$$

where $\boldsymbol{\mathcal{A}}$ is an auxiliary quantity needed to close the EOM. The driving terms $\boldsymbol{\Psi}^e$ and $\boldsymbol{\Psi}^b$ are functionals of $\rho^<$ and $\boldsymbol{\gamma}^<$. They have been already encountered in Refs. [16,17] in the context of the simpler *GW* and *GD* approximations. In particular,

$$\boldsymbol{\Psi}^e(t) \equiv \boldsymbol{\rho}^>(t)\boldsymbol{v}(t)\boldsymbol{\rho}^<(t) - \boldsymbol{\rho}^<(t)\boldsymbol{v}(t)\boldsymbol{\rho}^>(t), \tag{10}$$

$$\boldsymbol{\Psi}^b(t) \equiv \boldsymbol{\gamma}^>(t)\boldsymbol{g}(t)\boldsymbol{\rho}^<(t) - \boldsymbol{\gamma}^<(t)\boldsymbol{g}(t)\boldsymbol{\rho}^>(t), \tag{11}$$

and $\boldsymbol{h}^e_{\rm eff} = \boldsymbol{h}^e - \boldsymbol{\rho}^\Delta\boldsymbol{v}$ with $\boldsymbol{\rho}^\Delta = \boldsymbol{\rho}^> - \boldsymbol{\rho}^<$. The matrices $\boldsymbol{h}^e$ and $\boldsymbol{\rho}^\lessgtr$ in the two-electron space (hence represented by boldface letters) are defined with elements $h^e_{\mu\nu} = h^e_{\substack{ij\\mn}} = h^e_{ij}\delta_{nm} - \delta_{ij}h^e_{nm}$ and $\rho^\lessgtr_{\mu\nu} = \rho^\lessgtr_{\substack{ij\\mn}} = \rho^\lessgtr_{ij}\rho^\gtrless_{nm}$.

Equations (1) and (9) together with the Ehrenfest equation for ϕ_μ, see below, form a system of seven first-order ODEs that can be conveniently solved numerically using a time-stepping algorithm. This is the first main result of our work. The $G\widetilde{W}^{(2)}$ approximation is easily derived by discarding terms of order higher than g^2. Taking into account that [50] $\boldsymbol{\mathcal{G}}^{eb} = \mathcal{O}(g^2)$, $\boldsymbol{\mathcal{G}}^b = \mathcal{O}(g)$, and $\boldsymbol{\mathcal{A}} = \mathcal{O}(g^2)$, the right-hand side of Eq. (9c) can be calculated with $\boldsymbol{g}\boldsymbol{\mathcal{G}}^e \to \boldsymbol{g}\boldsymbol{\mathcal{G}}^{ee}$ and $\boldsymbol{g}\boldsymbol{\mathcal{A}} \to 0$; this implies that in $G\widetilde{W}^{(2)}$ the EOM for $\boldsymbol{\mathcal{A}}$ decouples. We also observe that the EOM in the *GD* approximation, see Ref. [16], are recovered from the $G\widetilde{W}^{(2)}$ method upon setting $v = 0$ (in this case we are left with only the equation for $\boldsymbol{\mathcal{G}}^b$). The EOM in the *GW* approximation [17,18,20] are instead recovered from the full $G\widetilde{W}$ method upon setting $g = 0$ (in this case we are left with only the equation for $\boldsymbol{\mathcal{G}}^{ee}$).

Combining different methods. The treatment of pure electronic correlations is not limited to the *GW* approximation. By properly modifying the index order of the matrices $\boldsymbol{\mathcal{G}}^{ee}$, $\boldsymbol{\rho}^\lessgtr$, $\boldsymbol{h}^e$, and $\boldsymbol{v}$ in Eq. (9a) we can explore a large variety of methods [20]. They include the one-bubble or second-order direct (2B^d), second-order exchange (2B^x), *GW*, exchange-only *GW* (*XGW*), *GW* plus exchange (*GW* + *X*), *T*-matrix in the particle-hole channel (T^{ph}), exchange-only T^{ph} (XT^{ph}), T^{ph} plus exchange ($T^{ph} + X$), *T*-matrix in the particle-particle channel (T^{pp}), and exchange-only T^{pp} (XT^{pp}) [50]. Let "c" be the index for one of these correlated methods, and let us denote by $\mathcal{G}^{ee(c)}_{imjn}$ the corresponding two-particle GF. Different methods can be combined to *simultaneously* include several types of correlation effects if the full $\mathcal{G}^{ee}$ is evaluated according to

$$\mathcal{G}^{ee}_{imjn}(t) = \sum\nolimits_c n_c\mathcal{G}^{ee(c)}_{imjn}(t). \tag{12}$$

In the Supplemental Material [50] we discuss how to choose the integers n_c to avoid double countings. By decorating the electronic two-particle matrices $\boldsymbol{\rho}^\lessgtr$, $\boldsymbol{h}^e$, and $\boldsymbol{v}$ in the EOM for $\boldsymbol{\mathcal{G}}^{ee(c)}$ with the superscript c, the whole GKBA+ODE toolbox for interacting electrons and bosons can then be summarized as (omitting the dependence on the time variable)

$$i\frac{d}{dt}\phi_\mu = h^b_{\mu\nu}\phi_\nu + \sum\nolimits_{\nu,ij}\alpha_{\mu\nu}g_{\nu,ij}\rho_{ji}, \tag{13a}$$

$$i\frac{d}{dt}\rho^<_{lj} = \left\{\sum_i h^e_{li}\rho^<_{ij} - \sum_{imn} v_{lnmi}\left[\mathcal{G}^{ee}_{imjn} + s_1 d\mathcal{G}^{eb}_{imjn}\right] + d\sum_{\mu,i} g_{\mu,li}\,\mathcal{G}^b_{\mu,ij}\right\} - \{l \leftrightarrow j\}^*, \tag{13b}$$

$$i\frac{d}{dt}\gamma^<_{\mu\nu} = \left\{\sum_\beta h^b_{\mu\beta}\gamma^<_{\beta\nu} + d\sum_{\beta,mn}\alpha_{\mu\beta}g_{\beta,mn}\,\mathcal{G}^b_{\nu,nm}\right\} - \{\mu \leftrightarrow \nu\}^*, \tag{13c}$$

$$i\frac{d}{dt}\boldsymbol{\mathcal{G}}^{ee(c)} = -\boldsymbol{\Psi}^{e(c)} + \boldsymbol{h}^{e(c)}_{\rm eff}\boldsymbol{\mathcal{G}}^{ee(c)} - \boldsymbol{\mathcal{G}}^{ee(c)}\boldsymbol{h}^{e(c)\dagger}_{\rm eff}, \tag{13d}$$

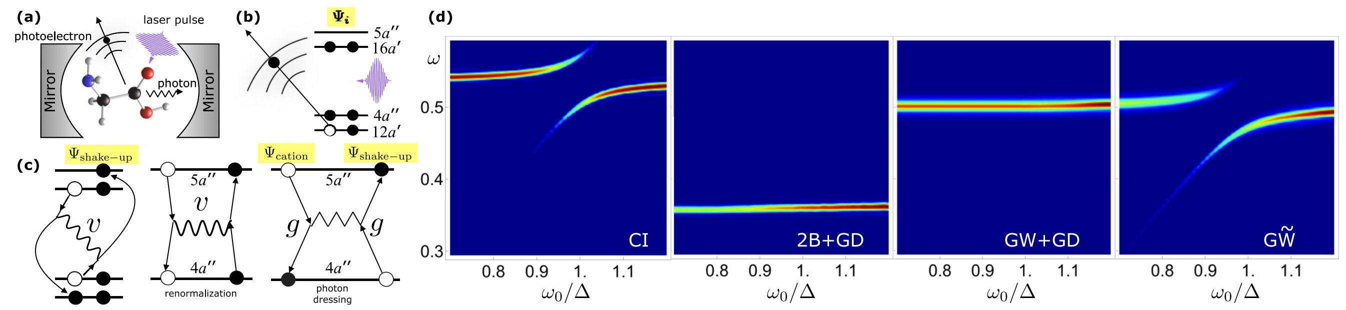

FIG. 2. (a) Illustration of the Gedanken experiment. A Gly molecule is ionized by a laser pulse and a cavity photon is emitted. (b) The four MOs involved in the charge migration of Gly when the electron is ionized from the $12a'$ MO. Electrons (black dots) on the MOs identify the state Ψ_i after ionization. (c) Shake-up process leading to state $\Psi_{\text{shake-up}}$ (left); scattering between electrons in the $4a''$ and $5a''$ MOs responsible for a sizable renormalization of the energy of the shake-up state (middle); electron-photon scattering leading to transition $\Psi_{\text{shake-up}} \leftrightarrow \Psi_{\text{cation}}$ (right). (d) Spectrograms of the occupancy of the $12a'$ MO in different schemes.

$$i\frac{d}{dt}\boldsymbol{\mathcal{G}}^{eb} = \boldsymbol{\rho}^{\Delta(GW)}\boldsymbol{g}^{\dagger}\boldsymbol{\mathcal{G}}^{b} - \boldsymbol{\mathcal{G}}^{b\dagger}\boldsymbol{g}\boldsymbol{\rho}^{\Delta(GW)} + \boldsymbol{h}^{e(GW)}_{\text{eff}}\boldsymbol{\mathcal{G}}^{eb} - \boldsymbol{\mathcal{G}}^{eb}\boldsymbol{h}^{e(GW)\dagger}_{\text{eff}}, \tag{13e}$$

$$i\frac{d}{dt}\boldsymbol{\mathcal{G}}^{b} = -\boldsymbol{\Psi}^{b} - s_1\boldsymbol{\alpha}\boldsymbol{g}[\boldsymbol{\mathcal{G}}^{ee(GW)} + s_2\boldsymbol{\mathcal{G}}^{eb}] - s_1 s_2\boldsymbol{\mathcal{A}}\boldsymbol{g}\boldsymbol{\rho}^{\Delta(GW)} + \boldsymbol{h}^{b}\boldsymbol{\mathcal{G}}^{b} - \boldsymbol{\mathcal{G}}^{b}[\boldsymbol{h}^{e(GW)} - s_1\boldsymbol{\rho}^{\Delta(GW)}\boldsymbol{v}^{(GW)}], \tag{13f}$$

$$i\frac{d}{dt}\boldsymbol{\mathcal{A}} = \boldsymbol{\mathcal{G}}^{b}\boldsymbol{g}^{\dagger}\boldsymbol{\alpha} - \boldsymbol{\alpha}\boldsymbol{g}\boldsymbol{\mathcal{G}}^{b\dagger} + \boldsymbol{h}^{b}\boldsymbol{\mathcal{A}} - \boldsymbol{\mathcal{A}}\boldsymbol{h}^{b}. \tag{13g}$$

The control parameters d, s_1, and s_2 refer to the treatment of *e-b* correlations. The Ehrenfest approximation is recovered for $d = 0$ — in this case the only equations to solve are those for the displacements and momenta, i.e., Eq. (13a), and the electronic equations (13b) and (13d). *e-b* correlations are included choosing $d = 1$. In this case we can set $(s_1, s_2) = (0, 0)$ (GD), $(s_1, s_2) = (1, 0)$ ($G\widetilde{W}^{(2)}$), and $(s_1, s_2) = (1, 1)$ ($G\widetilde{W}$). The number of equations (13d) depends on the chosen treatment of electronic correlations, i.e., on the values of n_c's. If $n_c = 0$ the corresponding $\boldsymbol{\mathcal{G}}^{ee(c)}$ is not needed. The only exception is for $c = GW$: if $s_1 = 1$ then the EOM for $\boldsymbol{\mathcal{G}}^{ee(GW)}$ must be solved even for $n_{GW} = 0$, see Eq. (13f). The GKBA+ODE toolbox in Eqs. (13) generalizes the one published in Ref. [14] in two ways: (i) it includes the $G\widetilde{W}^{(2)}$ and $G\widetilde{W}$ methods, and (2) it allows for combining different treatments of electronic correlations, for a total of 2^{12} distinct diagrammatic methods [50]. This is the second main result of our work.

Charge migration in a cavity. We consider the Gly I conformer of the glycine molecule and study the correlation-induced charge migration due to the removal of an electron from the $12a'$ molecular orbital (MO), see Fig. 2(b). In free space this case has been investigated at length [20,51–54]. Coulomb interaction is responsible for a *shake-up* process where an electron from the $16a'$ MO fills the photo-hole and another electron is promoted from the $4a''$ MO to the initially empty $5a''$ MO, left of Fig. 2(c). We refer to our previous works for the electronic structure and basis representation [54,55]. In Ref. [20] we showed that the energy of the shake-up state is strongly *renormalized* by the exchange interaction between electrons in the $4a''$ and $5a''$ MOs, middle of Fig. 2(c), and that capturing this renormalization requires a GW treatment. Here we analyze how the dynamics is affected by a single cavity mode that couples the shake-up state $\Psi_{\text{shake-up}}$ to the lowest-energy cationic state Ψ_{cation} (one hole in $16a'$ MO), right of Fig. 2(c).

Let $\Delta = E_{\text{shake-up}} - E_i = 0.522$ a.u. be the energy difference between $\Psi_{\text{shake-up}}$ and the state Ψ_i of Gly just after photoionization. In Fig. 2(d) we show the Fourier transform of the occupancy of the $12a'$ MO for different frequencies ω_0 of the cavity mode. The coupling $g = \lambda d_{4a'',5a''}\sqrt{\omega_0}$ is proportional to the dipole moment $d_{4a'',5a''}$ between the MOs involved in the transition $\Psi_{\text{shake-up}} \to \Psi_{\text{cation}}$. The electron-photon coupling strength λ is determined by the mode wave function at the location of the molecule [56]. We take $d_{4a'',5a''} = 0.125$ a.u. as the average dipole moment along three orthogonal directions and choose $\lambda = 0.212$ a.u. Details on the numerical simulations can be found in the Supplemental Material [50].

The first panel of Fig. 2(d) displays the configuration interaction (CI) spectrogram. For $\omega_0 \ll \Delta$ cavity photons are hardly emitted and the only possible transition is $\Psi_i \leftrightarrow \Psi_{\text{shake-up}}$. Correspondingly, the spectrum has only one peak at frequency $\Delta_{\text{CI}} = 0.544$ a.u. $\simeq \Delta$. As ω_0 approaches Δ, an Autler-Townes doublet of entangled electron-photon many-body states becomes visible [57,58]. It is due to the *photon dressing* of the cationic state which makes the transition $\Psi_i \leftrightarrow \Psi_{\text{cation}}$ bright and dominant when $\omega_0 > \Delta$.

For a diagrammatic approximation to reproduce CI, the electronic self-energy must account for all three mechanisms illustrated in Fig. 2(c). In the second panel of Fig. 2(d) we report the 2B+GD spectrogram. This approximation captures only the shake-up process, thereby yielding a ω_0-independent structure at energy $\Delta_{\text{2B}} = 0.356$ a.u. As expected [20], the $GW + GD$ method renormalizes Δ_{2B} to $\Delta_{GW} = 0.503 \simeq \Delta_{\text{2B}} + 2v^{x}_{4a'',5a''}$, see third panel, where $v^{x}_{4a'',5a''} = 0.08$ a.u. is the exchange Coulomb integral responsible for the scattering in Fig. 2(c) (middle). Achieving the CI value Δ calls for vertex corrections which, however, are beyond the current

GKBA+ODE formulation. The most severe deficiency of the $GW + GD$ spectrogram is the absence of the Autler-Townes doublet. In fact, photon dressing requires a nonperturbative treatment in the e-b coupling like the $G\widetilde{W}$ method. The $G\widetilde{W}$ spectrogram is shown in the fourth panel. Although the intensity of the low-ω_0 peak is weaker than in CI, the improvement over $GW + GD$ is quantitatively and qualitatively substantial.

In conclusion, we have extended the time-linear GKBA+ODE formulation for interacting fermions and bosons to the doubly screened $G\widetilde{W}$ method and shown how to combine different diagrammatic approximations to account for multiple correlation effects simultaneously while preserving all conserving properties. The case of correlation-induced charge migration of glycine in an optical cavity exemplifies the superiority of $G\widetilde{W}$ over current state-of-the-art approaches. We emphasize that the scaling of a $G\widetilde{W}$ calculation with the system size is the same as for GW, thus making the method potentially available for real-time first-principles simulations of finite [20,55] and extended [19,59] systems. Last but not least, the GKBA+ODE formulation lends itself to studies of multiscale phenomena through the implementation of adaptive time-stepping algorithms.

Acknowledgments. We acknowledge the financial support from MIUR PRIN (Grant No. 20173B72NB), from INFN through the TIME2QUEST project, and from Tor Vergata University through the Beyond Borders Project ULEXIEX. We also acknowledge useful discussions with Andrea Marini.

[1] R. P. Feynman, Space-time approach to quantum electrodynamics, Phys. Rev. **76**, 769 (1949).

[2] A. A. Abrikosov, L. P. Gor'kov, and I. E. Dzialoshinskii, *Methods of Quantum Field Theory in Statistical Physics* (Dover Publications, New York, 1975)

[3] R. D. Mattuck, *A Guide to Feynman Diagrams in the Many-Body Problem*, 2nd ed. (Dover Publications, New York, 1992).

[4] A. Fetter and J. Walecka, *Quantum Theory of Many-Particle Systems*, Dover Books on Physics (Dover Publications, New York, 2003).

[5] E. K. U. Gross, E. Runge, and O. Heinonen, *Many-Particle Theory* (A. Hilger, London, 1991).

[6] O. V. Konstantinov and V. I. Perel, A diagram technique for evaluating transport quantities, Sov. Phys. JETP **12**, 142 (1961).

[7] L. V. Keldysh, Diagram technique for nonequilibrium processes, Sov. Phys. JETP **20**, 1018 (1965).

[8] L. Kadanoff and G. Baym, *Quantum Statistical Mechanics Green's Function Methods in Equilibrium and Nonequilibrium Problems* (W.A. Benjamin, New York, 1962).

[9] G. Stefanucci and R. van Leeuwen, *Nonequilibrium Many-Body Theory of Quantum Systems: A Modern Introduction* (Cambridge University Press, Cambridge, England, 2013).

[10] A. Stan, N. E. Dahlen, and R. van Leeuwen, Time propagation of the Kadanoff-Baym equations for inhomogeneous systems, J. Chem. Phys. **130**, 224101 (2009).

[11] K. Balzer and M. Bonitz, *Nonequilibrium Green's function Approach to Inhomogeneous Systems*, Lecture Notes in Physics No. 867 (Springer, Heidelberg, 2013).

[12] M. Schüler, J. Berakdar, and Y. Pavlyukh, Time-dependent many-body treatment of electron-boson dynamics: Application to plasmon-accompanied photoemission, Phys. Rev. B **93**, 054303 (2016).

[13] M. Schüler, D. Golež, Y. Murakami, N. Bittner, A. Herrmann, H. U. Strand, P. Werner, and M. Eckstein, NESSi: The non-equilibrium systems simulation package, Comput. Phys. Commun. **257**, 107484 (2020).

[14] Y. Pavlyukh, E. Perfetto, D. Karlsson, R. van Leeuwen, and G. Stefanucci, Time-linear scaling nonequilibrium Green's function method for real-time simulations of interacting electrons and bosons. II. Formalism, Phys. Rev. B **105**, 125134 (2022).

[15] P. Lipavský, V. Špička, and B. Velický, Generalized Kadanoff-Baym ansatz for deriving quantum transport equations, Phys. Rev. B **34**, 6933 (1986).

[16] D. Karlsson, R. van Leeuwen, Y. Pavlyukh, E. Perfetto, and G. Stefanucci, Fast Green's Function Method for Ultrafast Electron-Boson Dynamics, Phys. Rev. Lett. **127**, 036402 (2021).

[17] N. Schlünzen, J.-P. Joost, and M. Bonitz, Achieving the Scaling Limit for Nonequilibrium Green Functions Simulations, Phys. Rev. Lett. **124**, 076601 (2020).

[18] J.-P. Joost, N. Schlünzen, and M. Bonitz, G1-G2 scheme: Dramatic acceleration of nonequilibrium Green functions simulations within the Hartree-Fock generalized Kadanoff-Baym ansatz, Phys. Rev. B **101**, 245101 (2020).

[19] E. Perfetto, Y. Pavlyukh, and G. Stefanucci, Real-Time GW: Toward an *Ab Initio* Description of the Ultrafast Carrier and Exciton Dynamics in Two-Dimensional Materials, Phys. Rev. Lett. **128**, 016801 (2022).

[20] Y. Pavlyukh, E. Perfetto, and G. Stefanucci, Photoinduced dynamics of organic molecules using nonequilibrium Green's functions with second-Born, GW, T-matrix, and three-particle correlations, Phys. Rev. B **104**, 035124 (2021).

[21] T. Frederiksen, M. Paulsson, M. Brandbyge, and A.-P. Jauho, Inelastic transport theory from first principles: Methodology and application to nanoscale devices, Phys. Rev. B **75**, 205413 (2007).

[22] E. Cannuccia and A. Marini, Effect of the Quantum Zero-Point Atomic Motion on the Optical and Electronic Properties of Diamond and Trans-Polyacetylene, Phys. Rev. Lett. **107**, 255501 (2011).

[23] Y. Pavlyukh, E. Perfetto, D. Karlsson, R. van Leeuwen, and G. Stefanucci, Time-linear scaling nonequilibrium Green's function method for real-time simulations of interacting electrons and bosons. II. Dynamics of polarons and doublons, Phys. Rev. B **105**, 125135 (2022).

[24] V. Rizzi, T. N. Todorov, J. J. Kohanoff, and A. A. Correa, Electron-phonon thermalization in a scalable method for real-time quantum dynamics, Phys. Rev. B **93**, 024306 (2016).

[25] G. Baym and L. P. Kadanoff, Conservation laws and correlation functions, Phys. Rev. **124**, 287 (1961).

[26] G. Baym, Self-consistent approximations in many-body systems, Phys. Rev. **127**, 1391 (1962).

[27] R. van Leeuwen, First-principles approach to the electron-phonon interaction, Phys. Rev. B **69**, 115110 (2004).
[28] D. Karlsson and R. van Leeuwen, Non-equilibrium Green's functions for coupled fermion-boson systems, in *Handbook of Materials Modeling*, edited by W. Andreoni and S. Yip (Springer International Publishing, Cham, 2020), pp. 367–395.
[29] D. Sangalli and A. Marini, Ultra-fast carriers relaxation in bulk silicon following photoexcitation with a short and polarized laser pulse, Europhys. Lett. **110**, 47004 (2015).
[30] A. Molina-Sánchez, D. Sangalli, L. Wirtz, and A. Marini, Ab initio calculations of ultrashort carrier dynamics in two-dimensional materials: Valley depolarization in single-layer WSe_2, Nano Lett. **17**, 4549 (2017).
[31] M. Selig, G. Berghäuser, A. Raja, P. Nagler, C. Schüller, T. F. Heinz, T. Korn, A. Chernikov, E. Malic, and A. Knorr, Excitonic linewidth and coherence lifetime in monolayer transition metal dichalcogenides, Nat. Commun. **7**, 13279 (2016).
[32] C. Trovatello, H. P. C. Miranda, A. Molina-Sánchez, R. Borrego-Varillas, C. Manzoni, L. Moretti, L. Ganzer, M. Maiuri, J. Wang, D. Dumcenco, A. Kis, L. Wirtz, A. Marini, G. Soavi, A. C. Ferrari, G. Cerullo, D. Sangalli, and S. D. Conte, Strongly coupled coherent phonons in single-layer MoS_2, ACS Nano **14**, 5700 (2020).
[33] J. Flick, C. Schäfer, M. Ruggenthaler, H. Appel, and A. Rubio, Ab initio optimized effective potentials for real molecules in optical cavities: Photon contributions to the molecular ground state, ACS Photonics **5**, 992 (2018).
[34] O. S. Ojambati, R. Chikkaraddy, W. D. Deacon, M. Horton, D. Kos, V. A. Turek, U. F. Keyser, and J. J. Baumberg, Quantum electrodynamics at room temperature coupling a single vibrating molecule with a plasmonic nanocavity, Nat. Commun. **10**, 1049 (2019).
[35] C. Schäfer, M. Ruggenthaler, H. Appel, and A. Rubio, Modification of excitation and charge transfer in cavity quantum-electrodynamical chemistry, Proc. Natl. Acad. Sci. USA **116**, 4883 (2019).
[36] X. Li, A. Mandal, and P. Huo, Cavity frequency-dependent theory for vibrational polariton chemistry, Nat. Commun. **12**, 1315 (2021).
[37] D. Karlsson, R. van Leeuwen, E. Perfetto, and G. Stefanucci, The generalized Kadanoff-Baym ansatz with initial correlations, Phys. Rev. B **98**, 115148 (2018).
[38] E. V. n. Boström, A. Mikkelsen, C. Verdozzi, E. Perfetto, and G. Stefanucci, Charge separation in donor-C_{60} complexes with real-time Green functions: The importance of nonlocal correlations, Nano Lett. **18**, 785 (2018).
[39] E. Perfetto, D. Sangalli, A. Marini, and G. Stefanucci, Ultrafast charge migration in XUV photoexcited phenylalanine: A first-principles study based on real-time nonequilibrium Green's functions, J. Phys. Chem. Lett. **9**, 1353 (2018).
[40] Y. Murakami, N. Tsuji, M. Eckstein, and P. Werner, Nonequilibrium steady states and transient dynamics of conventional superconductors under phonon driving, Phys. Rev. B **96**, 045125 (2017).
[41] H. Y. Fan, Temperature dependence of the energy gap in semiconductors, Phys. Rev. **82**, 900 (1951).
[42] Y. Murakami, P. Werner, N. Tsuji, and H. Aoki, Multiple amplitude modes in strongly coupled phonon-mediated superconductors, Phys. Rev. B **93**, 094509 (2016).
[43] F. Giustino, M. L. Cohen, and S. G. Louie, Electron-phonon interaction using Wannier functions, Phys. Rev. B **76**, 165108 (2007).
[44] A. Marini, S. Poncé, and X. Gonze, Many-body perturbation theory approach to the electron-phonon interaction with density-functional theory as a starting point, Phys. Rev. B **91**, 224310 (2015).
[45] O. D. Restrepo, K. Varga, and S. T. Pantelides, First-principles calculations of electron mobilities in silicon: Phonon and Coulomb scattering, Appl. Phys. Lett. **94**, 212103 (2009).
[46] C. Verdi, F. Caruso, and F. Giustino, Origin of the crossover from polarons to Fermi liquids in transition metal oxides, Nat. Commun. **8**, 15769 (2017).
[47] G. Mahan, *Many-Particle Physics*, 3rd ed. (Springer, US, New York, 2000).
[48] F. Giustino, Electron-phonon interactions from first principles, Rev. Mod. Phys. **89**, 015003 (2017).
[49] F. Caruso, M. Hoesch, P. Achatz, J. Serrano, M. Krisch, E. Bustarret, and F. Giustino, Nonadiabatic Kohn Anomaly in Heavily Boron-Doped Diamond, Phys. Rev. Lett. **119**, 017001 (2017).
[50] See Supplemental Material at http://link.aps.org/supplemental/10.1103/PhysRevB.106.L201408 for the derivation of the GKBA form of $\mathcal{G}^e$ and $\mathcal{G}^b$, the derivation of the EOM of $\mathcal{G}^e$ and $\mathcal{G}^b$, an exhaustive discussion on the different diagrammatic methods and how to combine them, and for numerical details of the time-dependent simulations.
[51] A. I. Kuleff, J. Breidbach, and L. S. Cederbaum, Multielectron wave-packet propagation: General theory and application, J. Chem. Phys. **123**, 044111 (2005).
[52] A. I. Kuleff and L. S. Cederbaum, Charge migration in different conformers of glycine: The role of nuclear geometry, Chem. Phys. **338**, 320 (2007).
[53] B. Cooper and V. Averbukh, Single-Photon Laser-Enabled Auger Spectroscopy for Measuring Attosecond Electron-Hole Dynamics, Phys. Rev. Lett. **111**, 083004 (2013).
[54] E. Perfetto, D. Sangalli, M. Palummo, A. Marini, and G. Stefanucci, First-principles nonequilibrium green's function approach to ultrafast charge migration in glycine, J. Chem. Theory Comput. **15**, 4526 (2019).
[55] E. Perfetto and G. Stefanucci, CHEERS: A tool for correlated hole-electron evolution from real-time simulations, J. Phys.: Condens. Matter **30**, 465901 (2018).
[56] J. Yang, Q. Ou, Z. Pei, H. Wang, B. Weng, Z. Shuai, K. Mullen, and Y. Shao, Quantum-electrodynamical time-dependent density functional theory within Gaussian atomic basis, J. Chem. Phys. **155**, 064107 (2021).
[57] S. H. Autler and C. H. Townes, Stark effect in rapidly varying fields, Phys. Rev. **100**, 703 (1955).
[58] E. Perfetto and G. Stefanucci, Some exact properties of the nonequilibrium response function for transient photoabsorption, Phys. Rev. A **91**, 033416 (2015).
[59] D. Sangalli, A. Ferretti, H. Miranda, C. Attaccalite, I. Marri, E. Cannuccia, P. Melo, M. Marsili, F. Paleari, A. Marrazzo, G. Prandini, P. Bonfà, M. O. Atambo, F. Affinito, M. Palummo, A. Molina-Sánchez, C. Hogan, M. Grüning, D. Varsano, and A. Marini, Many-body perturbation theory calculations using the YAMBO code, J. Phys.: Condens. Matter **31**, 325902 (2019).